AFRL-SR-AR-TR-04-

0620

REPORT DOCUMENTATION PAGE

1. REPORT DATE (DD-MM-YYYY)	2. REPORT TYPE	3. DATES COVERED (From - To)
14-10-2004	Final Technical Report	15-12-2004

4. TITLE AND SUBTITLE
STTR Phase I: 2.3 Micron High Power Continuous Wave Diode Laser Arrays

5a. CONTRACT NUMBER
FA9550-04-C-0021

5b. GRANT NUMBER

5c. PROGRAM ELEMENT NUMBER

6. AUTHOR(S)
David Westerfeld

5d. PROJECT NUMBER

5e. TASK NUMBER

5f. WORK UNIT NUMBER

7. PERFORMING ORGANIZATION NAME(S) AND ADDRESS(ES)

Power Photonic Corporation
Room 214 Old Chemistry Bldg.
SUNY Stony Brook
Stony Brook, NY 11794-3717

8. PERFORMING ORGANIZATION REPORT NUMBER
23STTR4

9. SPONSORING / MONITORING AGENCY NAME(S) AND ADDRESS(ES)
USAF, AFRL
AF Office Scientific Research
4015 Wilson Blvd Room 713
Arlington VA 22203-1954

NE

10. SPONSOR/MONITOR'S ACRONYM(S)
AFOSR

11. SPONSOR/MONITOR'S REPORT NUMBER(S)

12. DISTRIBUTION / AVAILABILITY STATEMENT
Approved for public release; distribution unlimited.

13. SUPPLEMENTARY NOTES

14. ABSTRACT
Report developed under STTR contract for topic AF03T025 (2.3 Micron High Power Continuous Wave Diode Laser Arrays). This final technical report describes progress made to demonstrate the technical feasibility of high power GaSb based semiconductor laser arrays. These arrays have many potential applications including infrared countermeasures (IRCM), pumping of solid state lasers, low probability of intercept communication links, and trace gas analysis. Civilian applications exist in the fields of medical diagnostics and dermatological treatments. The research involved the fabrication and complete characterization of single emitter GaSb based devices. Successful results with the single emitter devices led to the demonstration, for the first time, of a one-dimensional 2.3 micron laser array. The array produced 10 watts in continuous wave operation, 18.5W in long pulse operation, and over 20W in short pulse operation (short pulse power limited by current source).

15. SUBJECT TERMS
STTR Report

16. SECURITY CLASSIFICATION OF:			17. LIMITATION OF ABSTRACT	18. NUMBER OF PAGES	19a. NAME OF RESPONSIBLE PERSON
a. REPORT	b. ABSTRACT	c. THIS PAGE			David Westerfeld
Unclassified	Unclassified	Unclassified		14	19b. TELEPHONE NUMBER (include area code) 631 632 1358

1 Introduction

This report documents the research activities carried out by Power Photonic Corporation and its university partner, the State University of New York at Stony Brook on the United States Air Force STTR entitled "2.3 Micron High Power Continuous Wave Diode Laser Arrays". Work performed as part of this Phase I effort demonstrated the technical feasibility of these semiconductor laser arrays by producing devices which greatly exceeded all of the original Phase I technical objectives. These early research devices provided powers far in excess of what has previously been available from semiconductor lasers in this important wavelength region. Further, the Phase I research indicated a path for future work that will lead to devices with even higher output power, efficiency, and beam quality.

Electrically pumped semiconductor lasers are preferred for their small size, high output power, ruggedness, low cost, and especially, their high energy conversion (wall-plug) efficiency. In the wavelength and power regions where semiconductor lasers are available, they have generally become the preferred type of laser source for most general purpose applications. Our goal in this research is to extend the range of military and civilian applications that can be filled by high efficiency semiconductor sources. We have increased the application range by producing, for the first time in the world, high power 2.3 μm semiconductor laser arrays. These arrays have demonstrated a room temperature continuous wave (cw) output power of 10 W from a 1 cm 20% fill factor laser bar. Under quasi-continuous wave (qcw) operation (30 μs pulse width, 300 Hz pulse repetition frequency), the output power was 18.5 W. Output power under short pulsed operation exceeded 20 W at the highest current we applied; even at 20 W the output power was still increasing linearly with current.

The devices described in this report operate near 2.3 μm. One advantage of these type-I lasers is the relative ease with which different wavelengths can be produced through comparatively small design refinements. High power lasers using a similar Type-I design have been demonstrated by SUNY Stony Brook operating up to 2.8 μm [1,2]. Lower powers have been demonstrated from devices operating at 2.9 μm. The combination of increased output power and a wider available range of output wavelengths has considerably expanded the application opportunities available to semiconductor lasers.

Potential applications for these devices cover a wide range, from dermatological, to medical diagnostic, trace gas sensing, and free space communication. The key applications we considered during this STTR were in the field of infrared countermeasures (IRCM). The devices can be employed either directly as high power band I sources, or for the optical pumping of band II sources. Band II sources, whether they be traditional solid state lasers or the new optically pumped semiconductor lasers (OPSL) developed by the Air Force Research Lab [3], benefit from the decreased heating and improved efficiency that can be provided by the laser arrays developed under this STTR.

2 Research Objectives

Our goals in Phase I were first to design, grow, and completely characterize single emitter lasers. Based on the results from these single emitter lasers, we intended to design and fabricate a high power laser array. We anticipated an array output power of ~5 watts in continuous wave operation.

Details of the results are presented in the Results section below. The synopsis is that the high temperature stability observed in the single emitter lasers, combined with a new analytic method we developed [4] for determining thermal fields in the laser array allowed us to increase the laser bar fill factor from 10% to 20%. This doubling of the fill factor, made possible by the thermal stability of our laser structure, allowed us to produce twice the anticipated array output power.

Success with our output power objective relatively early in the Phase I effort allowed us to go beyond our original Phase I goals, and perform and additional growth/processing step intended to further improve the device performance. An analysis of the Phase I results indicated that the wall plug efficiency of 11% could be significantly improved. We identified several promising areas where significant improvement in the wall plug efficiency could be obtained. We observed that the spontaneous emission emitted from the sides of the laser stripe did not pin at threshold, indicating that the carrier concentrations in parts of the device continued to increase after threshold. We attributed this increase in spontaneous emission to significant current spreading in the highly doped p-type cladding layer.

Devices were fabricated with a p-clad layer deeply etched to eliminate most of the material outside the laser stripe region. This etching step required the development of a successful dielectric and metallization deposition process before producing acceptable results. The etched single emitter devices tested exhibited a ~20% improvement in output power over the original devices, and no longer exhibited an increase of spontaneous emission above threshold.

The research objectives for Phase I were met and exceeded by large margins. Several promising approaches to significantly improve the wall plug efficiency of these devices are still open for future work.

3 Results

3.1 Initial 2.3 μm laser heterostructure simulations

3.1.1 Structure description

The laser heterostructure was designed with a broadened waveguide with low internal optical loss [5]. Figure 1 shows the laser heterostructure layer sequence and doping for growth by solid-source molecular-beam epitaxy. Heavily doped, compositionally graded, 40-nm-thick regions between the cladding layers and the n-GaSb substrate and the p^+-GaSb cap layer improve electron and hole conduction. The cladding layers are 2 μm-thick $Al_{0.9}Ga_{0.1}As_{0.07}Sb_{0.93}$. The p-cladding layer is Be-doped to 1 x 10^{18} cm^{-3} over the first 0.2 μm and to 5 x 10^{18} cm^{-3} over the remaining 1.8 μm. This was

done to reduce the internal optical loss caused by intervalance-band absorption in the p-cladding layer [6]. The total width of the $Al_{0.25}Ga_{0.75}As_{0.02}Sb_{0.98}$ broadened-waveguide layer is about 830 nm. The photoluminescence spectrum of the laser heterostructure wafer measured at room temperature is also shown in Figure 1.

cap p-GaSb 50nm Be: $2*10^{19}cm^{-3}$
grading p-GaSb/p-AlAsSb 40nm Be: $2*10^{19}cm^{-3}$
p-clad $Al_{0.9}Ga_{0.1}As_{0.07}Sb_{0.93}$ 1.8μm Be: $5*10^{18}cm^{-3}$
p-clad $Al_{0.9}Ga_{0.1}As_{0.07}Sb_{0.93}$ 200nm Be: $10^{18}cm^{-3}$
guide $Al_{0.25}Ga_{0.75}As_{0.02}Sb_{0.98}$ 300nm undoped
QW #2 $In_{0.41}Ga_{0.59}As_{0.14}Sb_{0.86}$ 11.5nm undoped
guide $Al_{0.25}Ga_{0.75}As_{0.02}Sb_{0.98}$ 200nm undoped
QW #1 $In_{0.41}Ga_{0.59}As_{0.14}Sb_{0.86}$ 11.5nm undoped
guide $Al_{0.25}Ga_{0.75}As_{0.02}Sb_{0.98}$ 300nm undoped
n-clad $Al_{0.9}Ga_{0.1}As_{0.07}Sb_{0.93}$ 2μm Te: $3*10^{17}cm^{-3}$
grading n-GaSb/n-AlAsSb 40nm Te: $10^{18}cm^{-3}$
buffer n-GaSb 500nm Te:$10^{18}cm^{-3}$
substrate n-GaSb

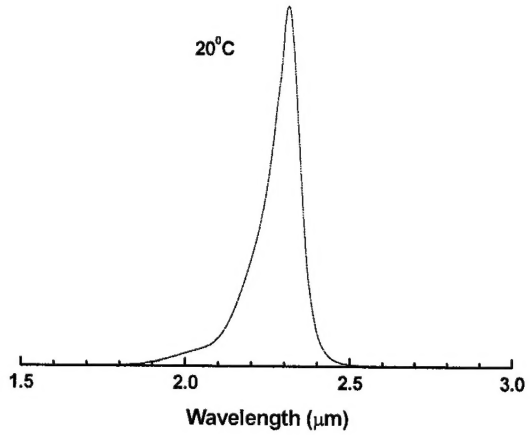

Figure 1. Layer sequence and room temperature photoluminescence spectrum.

The 1e-1hh transition energy with a maximum corresponding to 2.32 μm is close to the target wavelength. To achieve the required room temperature emission wavelength the QW width and composition were calculated based on the material parameters obtained from [7]. Special attention was given to increasing the separation between the first and second quantized electron states in QW to ensure stable single wavelength operation [8].

3.1.2 Optical field

Figure 2 shows the schematic band diagram under flat band conditions and the calculated optical field distribution. The overlap of the optical field with the doped cladding layers is below 15%, for low internal optical loss. Quaternary material refractive index values required for optical field calculations were obtained from [9].

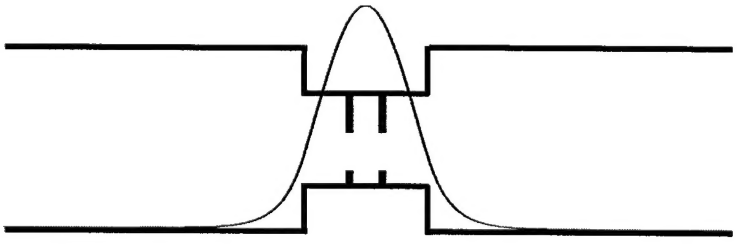

Figure 2. Schematic band diagram and calculated transverse near optical field intensity distribution.

Part of the wafer was processed into 100 μm-aperture, 1 mm-long, gain-guided lasers. Weak lateral current confinement was achieved by etching the p-cap layer outside of the current stripe and covering this area with ~200 nm of Si_3N_4. The facets were

coated to reflect 3% and 95%. The devices were In-soldered, epi-side down, onto copper heatsinks and characterized.

3.1.3 Carrier transport:

Figure 3 shows simulated band diagrams of two model laser heterostructures. The laser heterostructure models differ only in $Al_{0.25}Ga_{0.75}As_{0.02}Sb_{0.98}$ waveguide layer minority carrier lifetimes, namely 10 ns (a) and 0.1 ns (b).

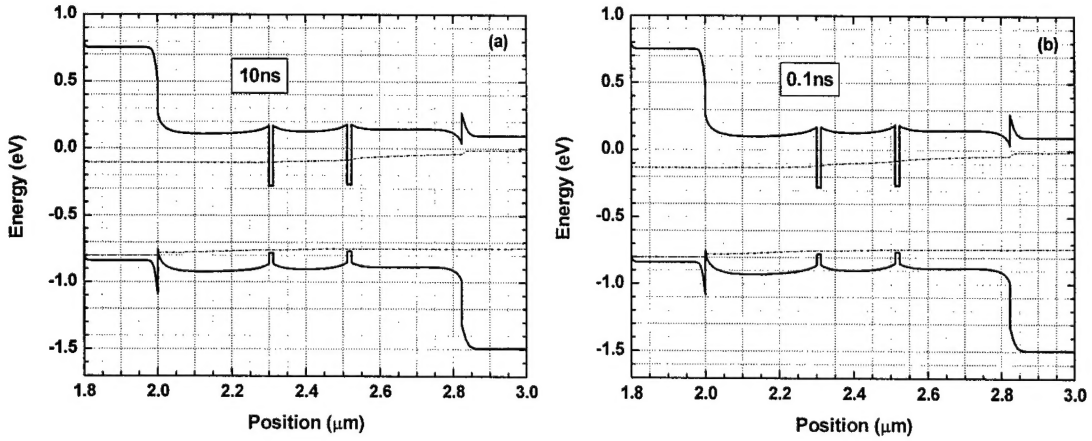

Figure 3. Simulated band diagrams of 2.3-μm laser heterostructure with 10ns (a) and 0.1ns (b) minority carrier lifetimes in waveguide layer. Band edges are shown by solid lines and quasi-Fermi levels by dash-dot lines.

Figure 3 reveals that the waveguide/cladding interface barriers for both electrons and holes are large enough to prevent excessive heterobarrier leakage carrier loss. Increasing the Al content of the waveguide layer to 35% should reduce recombination leakage but our modeling shows that it will also lead to an increase of the voltage drop across the laser heterostructure. The voltage drop associated with the barrier between the cladding and waveguide layers is responsible for the increase of the laser voltage and series resistance. From our simulation we conclude that the main contribution to the device series resistance comes from the transport of holes from p-cap GaSb layer to p-cladding $Al_{0.9}Ga_{0.1}As_{0.07}Sb_{0.93}$. This interface has large valence band offset. The heavily doped compositionally graded regions used in current design can be further optimized to minimize laser turn-on voltage and series resistance.

3.1.4 Heat transport:

Simulation of the heat transport in laser array was performed using a newly developed analytic approach [4] using parameters obtained experimentally. Figure 4 shows the lateral temperature profile calculated for CW operation and 1A of current per each 100-μm stripe.

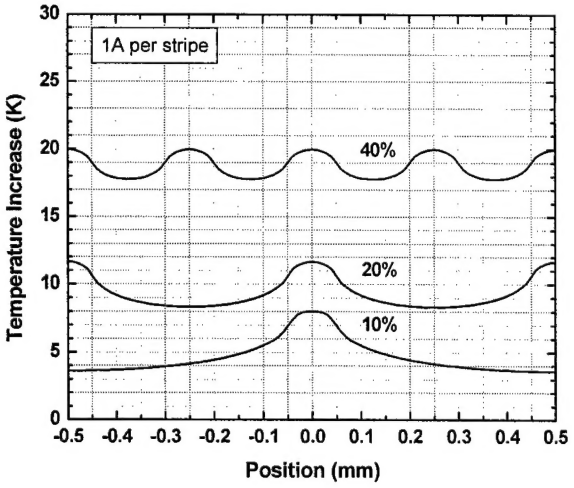

Figure 4. Simulated lateral temperature profile for 10, 20 and 40% fill-factor laser arrays packaged in microchannel cooled heatsinks.

3.2 Single emitter laser characterization

3.2.1 Output power versus current

Figure 5 shows CW output power and wall-plug efficiency versus current of a 2.3 μm 100 μm-wide 1mm-long AR/HR coated laser diode.

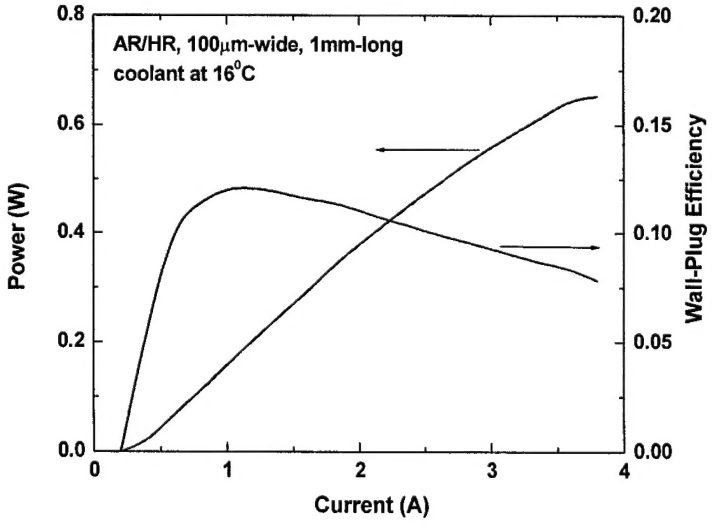

Figure 5. CW output power and wall-plug efficiency of single 2.3μm emitter.

The maximum CW output power is 650 mW and the wall-plug efficiency is ~11% at 1A. The threshold current is 360 mA the slope efficiency is 0.21 W/A and the differential quantum efficiency is 39%. Measurements of the device voltage–current characteristics were used to determine the device turn-on voltage (~ 0.8 V) and series resistance (~0.4 Ω).

3.2.2 Thermal performance

Figure 6 shows the threshold current and slope efficiency for a single 1 mm long by 100 μm wide broad area laser mounted epi side down on a copper heat sink as a function of temperature. The empirical characteristic temperature T_0, which describes the exponential dependence of threshold current on temperature, is 95 K. T_1, the empirical characteristic temperature for slope efficiency, is 183 K.

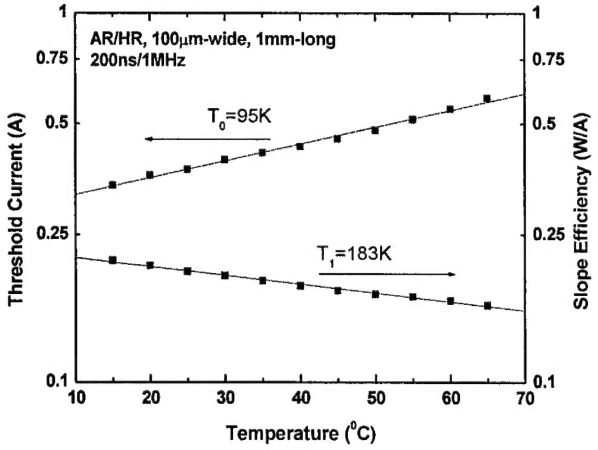

Figure 6: Semi-logarithmic graph showing threshold current and slope efficiency versus heat sink temperature.

3.2.3 Laser spectrum

Figure 7 shows the single laser spectra under both pulsed and CW operation. The peak laser wavelength increases with temperature from about 2.33 μm at 20 C up to 2.38 μm at 60 C due to band gap reduction with increasing temperature. The full-width, half-

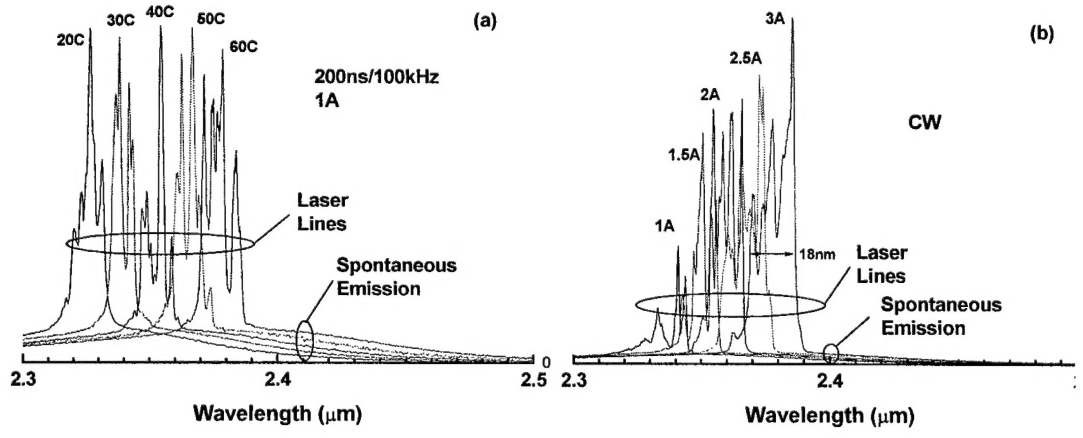

Figure 7: Laser spectra at several temperatures in pulsed (left) and CW (right) operation.

maximum (FWHM) spectral width is approximately 10 nm at a drive current of 1.5 A, broadening to 18 nm at a drive current of 3 A.

The total loss was determined using the Hakki-Paoli technique adapted for broad area devices. The total loss is 21 to 22 cm^{-1}, as indicated from the low energy side of the gain spectra shown in Figure 8. Allowing 18 cm^{-1} for the mirror loss in this 1 mm long, high reflection/anti-reflection coated device, the internal optical loss is 3 to 4 cm^{-1}.

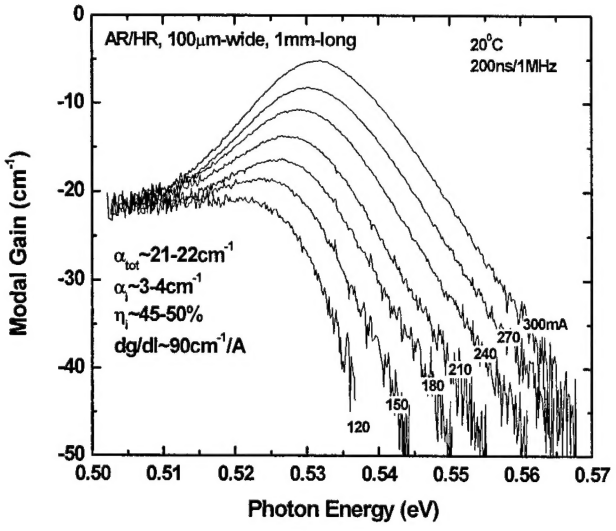

Figure 8: Hakki-Paoli gain spectra

The internal optical loss and the external efficiency can be used to calculate the internal efficiency, the fraction of pump current leading to photon generation. The internal efficiency for these devices is just 45 to 50%. This low internal efficiency can be partially explained by lateral current spreading, since no special steps were taken to ensure tight lateral current confinement.

3.2.4 Lateral current spread

An estimation of the lateral current spreading efficiency can be obtained by measuring the current dependence of the spontaneous emission intensity collected from the side of the laser stripe. With an indirect band gap waveguide, and with the assumption that the carrier concentration is pinned after threshold, any change in spontaneous emission intensity over threshold is due only to carrier spreading. Figure 9 presents the spectrally integrated spontaneous emission versus current. The pronounced change in slope at threshold allows us to calculate that the lateral current spreading efficiency is approximately 75%.

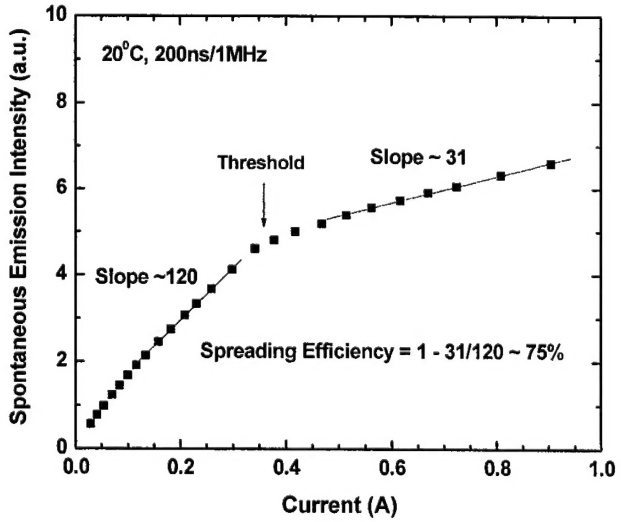

Figure 9: Integrated spontaneous emission versus current

3.3 Array performance

A laser bar was fabricated and soldered into a metallized groove in a watercooled microchannel BeO heat sink. The laser bar dimensions of 1 mm long by 1 cm wide were chosen to be compatible with the commercially available cooler. There were 19 individual 100 μm wide emitters evenly spaced along the bar with a center-to-center spacing of 500 μm (fill factor ~20%). As with the single emitter lasers, the front facets were anti-reflection (3%) coated and the back facets were high reflection (95%) coated.

3.3.1 Power and wall plug efficiency

The array produced 10 W of continuous wave power at a drive current of 70 A and a heat sink temperature of 18 C (see Figure 10). In pulsed operation, the output power continued to scale linearly with input current up to at least 100 A, where the array was producing ~20 W of output power. In the intermediate case of qCW operation with a pulse duration of 30 μs and a pulse repetition frequency of 300 Hz, the array demonstrated an output power of 18.5 W at 100 A input current and a heat sink temperature of 18 C. Continuous wave power output was limited by thermal rollover, qCW and pulsed output power was limited by the maximum permitted drive current of 100 A. The array spectrum (see the inset of Figure 10) was centered at 2.36 μm with spectral width of about 20 nm FWHM. The spectral shift indicates that the active region was about 75 C warmer than the heat sink at maximum CW power. Figure 5 also shows the wall plug efficiency, which peaked near 9% at a drive current of 30 A.

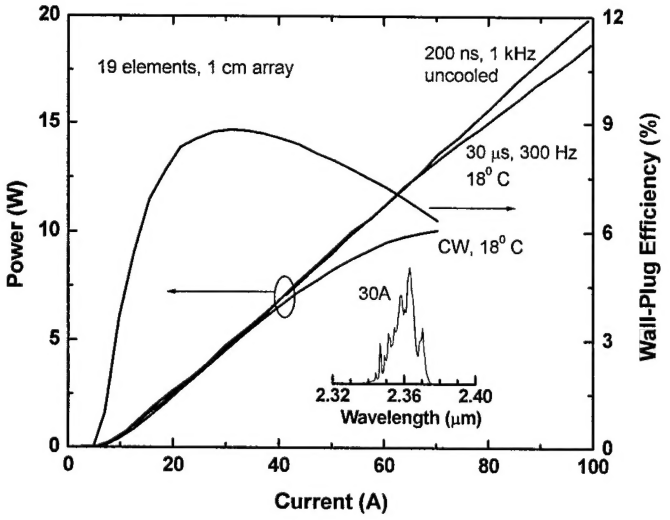

Figure 10: Laser array power and wall plug efficiency under cw, qcw and pulsed opration. The inset shows the array spectrum.

3.4 Reducing lateral current spreading

3.4.1 Power conversion efficiency

Our initial devices exhibited a CW power conversion efficiency of ~11% at 1A for single lasers and ~9% at 30A for a 19 element 1 cm-long array. The relatively low power-conversion efficiency is caused by an excessive voltage drop across the laser heterostructure and a low internal efficiency of ~50%. The excessive voltage drop

problem will be addressed in our proposed phase II development. Section 3.2.4 describes data indicating that lateral current spreading is significant and can reduce the device internal efficiency by about 25%.

3.4.2 Lateral current spread simulations

We performed 2D current transport simulations of the 2.3 μm laser heterostructure using the PADRE software package. To simplify the calculation we ignored the effect of the quantum wells (QWs) on carrier transport in the laser heterostructure and replaced the doped substrate and heavily doped substrate/n-clad superlattice by an ideal ohmic contact. The effect of current spreading in the thick 130 μm substrate layer is not significant since it does not influence the carrier distribution within the active layer. Figure 11a shows the device structure used in modeling.

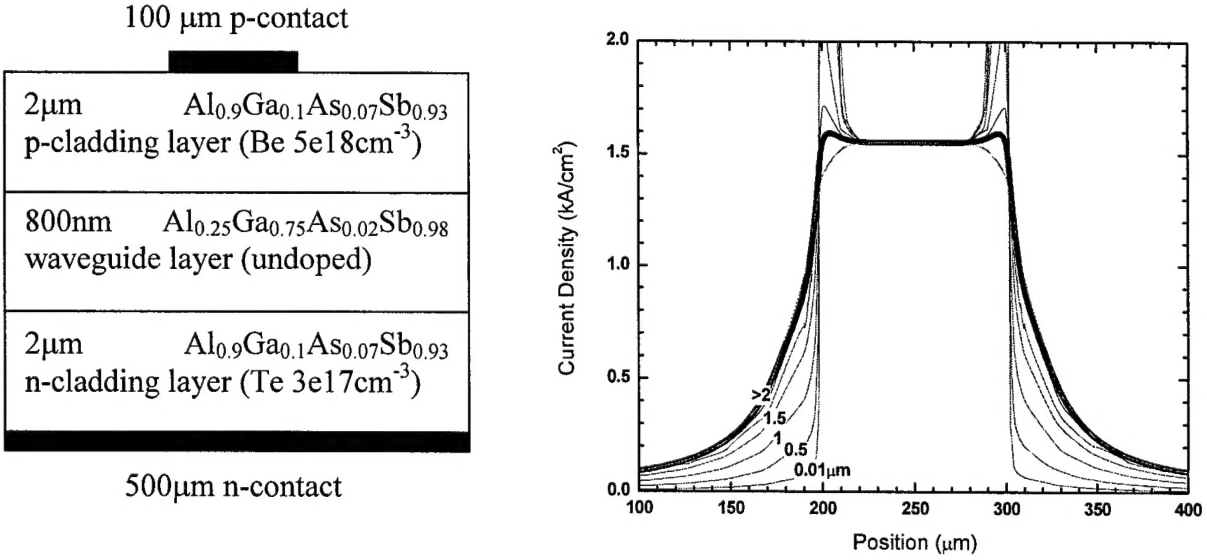

Figure 11. Laser structure model used in modeling (a) and dependence of the lateral current distribution on distance from p-contact (b).

Figure 11b shows the calculated current density in the lateral direction at several different distances from the p-contact. The current density maxima at the edges of the stripe are caused by the very high electric field at the sharp edges of the metal contact. Of greater concern are the long current density tails that indicate current spreading into the nominally unpumped regions between the laser stripes. The simulation confirms that the current spreading in the highly conductive 2 μm thick p-cladding layer is significant and that little additional current spreading occurs in the undoped waveguide. The simulation predicts that the laser internal efficiency is reduced by ~30% due to current spreading in the p-cladding layer.

Etching the heavily doped p-cladding layers outside of the contact stripe should greatly reduce the lateral leakage and thus increase the overall laser internal efficiency. Figure 12 shows simulation results obtained for a structure where the p-clad has been etched to 100 nm thick outside the laser stripe. Removal of the heavily doped regions leads to a substantial reduction of current spread at the QW location.

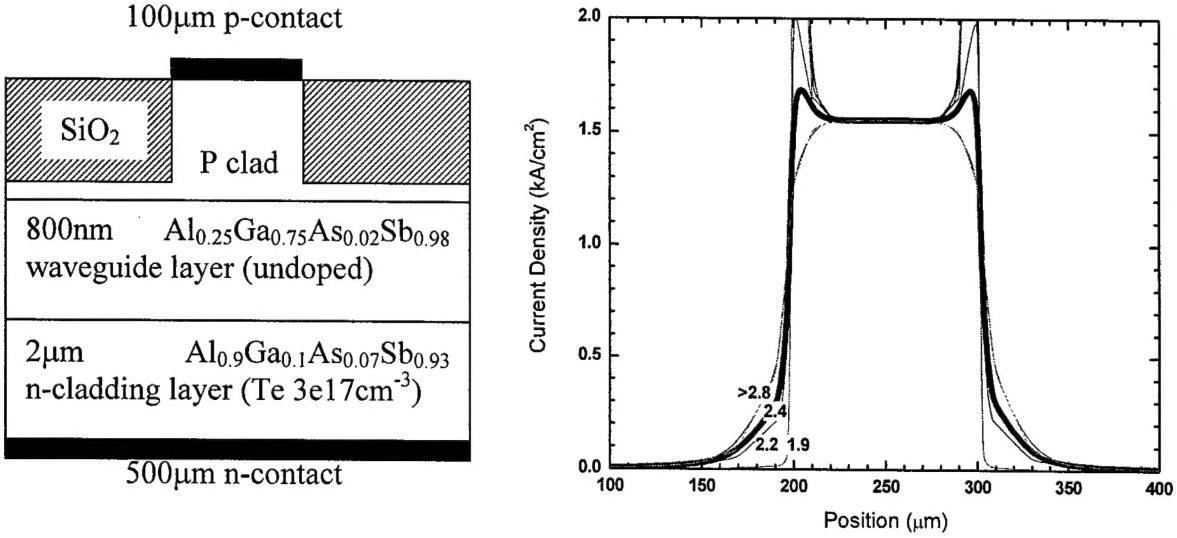

Figure 12. Laser structure model used in modeling (a) and dependence of the lateral current distribution on distance from p-contact (b).

3.4.3 Etched laser experiments for reducing lateral current spread

We performed experiments to test our approach for reducing lateral current spreading in 2.3μm GaSb-based lasers. Laser diodes with a design identical to the ones described above but with an etched p-clad were fabricated. Figure 13a shows the light-current characteristics of 1 mm-long 100 μm-wide AR/HR coated lasers processed with and without the etching step. In the etched device, the optical power level is increased by about 20% at the same current. Integrated spontaneous emission measured from the laser side (Figure 13b) is pinned at threshold in the etched devices but continues to grow in devices processed without the etching step.

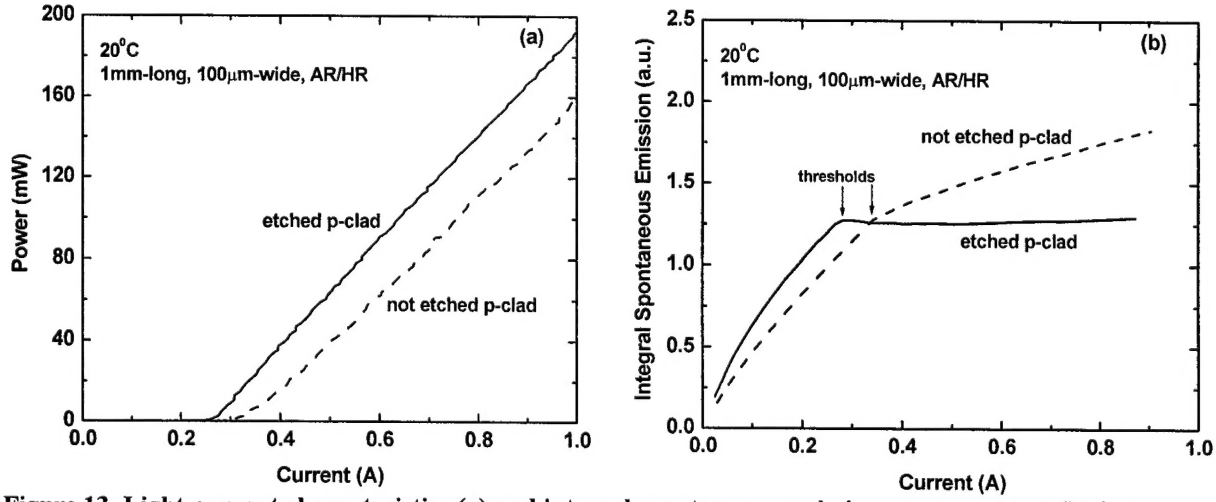

Figure 13. Light-current characteristics (a) and integral spontaneous emission versus current (b) for lasers with (solid) and without (dashed) etching of the p-cladding layer outside the current stripes.

We attribute the growth of the spontaneous emission intensity after threshold to carrier concentration increase in current spreading regions. Figure 13b data clearly indicate that the lateral current spreading is effectively suppressed by etching of the p-cladding material outside the current stripes. Total optical losses for the etched lasers were estimated from modal gain spectra measured using the Hakki-Paoli method (Figure 14a).

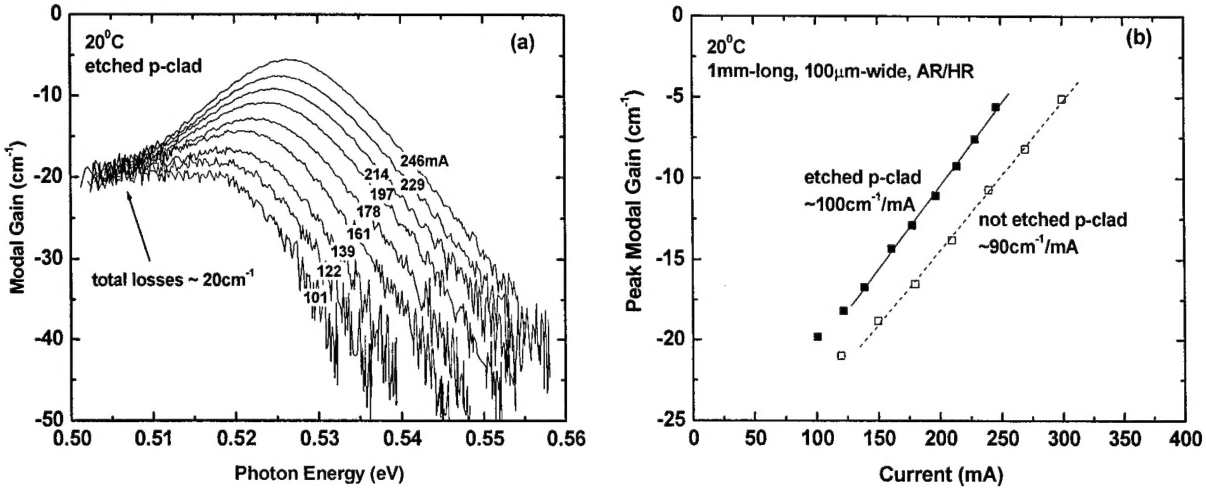

Figure 14. Current dependence of the modal gain spectra (a) and peak modal gain versus current (b) for lasers with (solid) and without (dashed) etching of the p-cladding outside the current stripes.

The optical losses stay nearly unchanged for devices processed with and without the etching step (compare Figure 8 and Figure 14a). The differential gain is improved in devices with the etched p-clad (Figure 14b).

Our preliminary experimental results demonstrate the feasibility of the approach chosen. Etching the p-cladding is an effective method to suppress the lateral current spreading in 2.3μm lasers, leading to improved device output power.

The etching process is not yet mature, with some difficulties experienced with the application of the dielectric and metallization layers. Improvements in the processing will be undertaken in Phase II to allow the successful processing of laser bar structures.

4 Technical Feasibility

Phase I research efforts are intended to demonstrate the technical feasibility of a proposed course of research. This Phase I is perhaps somewhat unusual in that we not only demonstrated feasibility on paper, we actually produced three generations of devices to unequivocally prove the practicality and potential of these devices. High output power at 2.3 μm was demonstrated from a compact, rugged semiconductor source. Deeply etched devices proved that the power conversion efficiency is subject to considerable improvements. Further large improvements in the wall plug efficiency remain to be demonstrated as part of a phase II effort.

5 Key Personnel

The following people have contributed to this STTR effort:

Power Photonic:

David Westerfeld

Gregory Belenky

Mikhail Kisin

Boris Laikhtman

SUNY Stony Brook:

Dmitri Donetski

Leon Shterengas

Alex Gourevitch

Sarnoff Corportation:

Ramon Martinelli

George Kim

6 Publications

This work has resulted in several publications and presentations:

Title: Thermal resistance and optimal fill factor of a high power diode laser bar
Authors: Laikhtman B, Gourevitch A, Donetsky D, Westerfeld D, Belenky G
Source: submitted Journal of Applied Physics

Title: 2.3 μm GaSb based linear laser array with 10 CW at room temperature
Authors: Belenky GL, Shterengas L, Gourevitch A, Donetsky D. Kim JG, Martinelli RU, Westerfeld D
Source: Solid State and Diode Laser Technology Review (SSDLTR), Albuquerque NM, 2004

Title: High-power 2.3 μm laser arrays emitting 10W CW at room temperature
Authors: Belenky GL, Kim JG, Shterengas L, Gourevitch A, Martinelli RU
Source: Electronics Letters 40 (12), 737, June 10 2004

Title: High-Power 2.3 μm GaSb-Based Linear Laser Array
Authors: Shterengas L, Belenky GL, Gourevitch A, Donetsky D, Kim JG,

Martinelli RU, Westerfeld D

Source: IEEE Photonics Technology Letters, 16 (10), 2218 - 2220, Oct. 2004

---

1 L. Shterengas, G.L. Belenky, J.G. Kim, R.U. Martinelli, "Design of high-power room-temperature continuous-wave GaSb-based type-I quantum-well lasers with lambda > 2.5 μm", *Semiconductor Sci. And Tech.* **19**, 655 (2004);

2 J.G. Kim, L. Shterengas, R.U. Martinelli, G.L. Belenky, "High-power room-temperature continuous wave operation of 2.7 and 2.8 μm In(Al)GaAsSb/GaSb diode lasers", *Appl. Phys. Lett.* **83**, 1926 (2003);

3 R. Kaspi, A. Ongstad, G.C. Dente, J. Chavez, M.L. Tilton, D. Gianardi, "High power and high brightness from an optically pumped InAs/InGaSb type-II midinfrared laser with low confinement", *Appl. Phys. Lett.* **81**, 406, (2002)

4 B. Laikhtman, A. Gourevitch, D. Donetsky, D. Westerfeld, G. Belenky "Current spread and overheating of high power laser bars", *J. Appl. Phys*, 3880, (2004)

5. J.G. Kim, L. Shterengas, R.U. Martinelli, G.L. Belenky, D.Z. Garbuzov, W.K. Chan, "Room-Temperature 2.5μm InGaAsSb/AlGaAsSb Diode Lasers Emitting 1W Continuous-Wave", *Appl. Phys. Lett.* **81**, 3146 (2002).

6. D.Z. Garbuzov, R.U. Martinelli, H. Lee, P.K. York, R.J. Menna, J.C. Connolly, S.Y. Narayan "Ultralow-loss broadened waveguide high-power 2μm AlGaAsSb/InGaAsSb/ GaSb separate-confinement quantum-well lasers", *Appl. Phys. Lett.* **69**, 2007 (1996); G.W. Turner, H.K. Choi, M.J. Manfra "Ultralow-threshold (50A/cm^2) strained single-quantum-well GaInAsSb/AlGaAsSb lasers emitting at 2.05μm", *Appl. Phys. Lett.* **72**, 876 (1998).

7. M.P.C.M. Krijn "Heterojunction band offsets and effective masses in III-V quaternary alloys", *Semicond. Sci. Technol.* **6**, 27 (1991).

8. D. V. Donetsky, D. Westerfeld, and G. L. Belenky, R. U. Martinelli, D. Z. Garbuzov, J. C. Connolly "Extraordinarily wide optical gain spectrum in 2.2–2.5 μm In(Al)GaAsSb/GaSb quantum-well ridge-waveguide lasers", *J. Appl. Phys.* **90**, 4281 (2001).

9. S. Adachi "Band gaps and refractive indexes of AlGaAsSb, GaInAsSb, and InPAsSb: key properties for a variety of the 2-4-μm optoelectronic device applications", *J. Appl. Phys.* **61**, 4869 (1987).